

Comparison of high-energy galactic and atmospheric tau neutrino flux

H. Athar^{1,2,*}, Kingman Cheung^{1,†}, Guey-Lin Lin^{2,‡}, Jie-Jun Tseng^{2,§}

¹*Physics Division, National Center for Theoretical Sciences, Hsinchu 300, Taiwan*

²*Institute of Physics, National Chiao Tung University, Hsinchu 300, Taiwan*

(Dated: November 2, 2018)

We compare the tau neutrino flux arising from the galaxy and the earth atmosphere for $10^3 \leq E/\text{GeV} \leq 10^{11}$. The intrinsic and oscillated tau neutrino fluxes from both sources are calculated. The intrinsic galactic ν_τ flux ($E \geq 10^3$ GeV) is calculated by considering the interactions of high-energy cosmic-rays with the matter present in our galaxy, whereas the oscillated galactic ν_τ flux is coming from the oscillation of the galactic ν_μ flux. For the intrinsic atmospheric ν_τ flux, we extend the validity of a previous calculation from $E \leq 10^6$ GeV up to $E \leq 10^{11}$ GeV. The oscillated atmospheric ν_τ flux is, on the other hand, rather suppressed. We find that, for $10^3 \leq E/\text{GeV} \leq 5 \cdot 10^7$, the oscillated ν_τ flux along the galactic plane dominates over the maximal intrinsic atmospheric ν_τ flux, i.e., the flux along the horizontal direction. We also briefly mention the presently envisaged prospects for observing these high-energy tau neutrinos.

PACS numbers: 95.85.Ry, 13.85.Tp, 98.38.-j, 14.60.Pq

I. INTRODUCTION

Searching for high-energy tau neutrinos ($E \geq 10^3$ GeV) will yield quite useful information about the highest energy phenomenon occurring in the universe [1]. The same search may also provide evidence for physics beyond the standard model [2]. The latter is suggested by the recent measurements of the atmospheric muon neutrino deficit, though yet there is no observation of oscillated atmospheric tau neutrinos at a significant confidence level [3]. Interestingly, it is also only recently that we have the first evidence of existence of tau neutrinos [4].

The high-energy tau neutrinos can be produced in pp and $p\gamma$ interactions taking place in cosmos. These interactions produce unstable hadrons that decay into tau neutrinos. In this paper, we mainly concentrate on pp interactions and will only briefly comment on $p\gamma$ interactions as source interactions for producing high-energy tau neutrinos. There can be several astrophysical sites where the pp interactions may occur. Examples of these include the relatively nearby and better known astrophysical sites such as our galaxy and the earth atmosphere, where the basic pp interactions occur as pA interactions. The pp interactions in these sites form a rather certain background to the extra-galactic high-energy tau neutrino searches. It is possible that such interactions are the only sources of high-energy tau neutrinos should the search for high-energy tau neutrinos originating from several proposed distant sites such as AGNs, GRBs, as well as groups and clusters of galaxies, turns out to be negative. Therefore, it is rather essential to investigate the high-energy tau neutrino flux expected from our galaxy and the earth atmosphere.

Both the galactic and atmospheric tau neutrinos can be categorized into intrinsic and oscillated ones. Here, intrinsic ν_τ flux refers to the ν_τ produced directly by an interaction while oscillated ν_τ refers to the ν_τ resulted from the $\nu_\mu \rightarrow \nu_\tau$ oscillation. Presently, there exists no estimate for the intrinsic high-energy ν_τ flux originating from our galaxy in pp interactions, although the estimates for ν_e and ν_μ fluxes due to the same interactions are available [5]. In this work, we calculate the intrinsic ν_τ flux from our galaxy by using the perturbative and nonperturbative QCD approaches to model the pp interactions, and taking into account all major tau neutrino production channels up to $E \leq 10^{11}$ GeV. We note that the production of tau neutrinos in the terrestrial context was discussed in Ref. [6], which uses a nonperturbative QCD approach for pp interactions. To calculate the oscillated galactic and atmospheric ν_τ fluxes, we apply the two-flavor neutrino oscillation analysis [3].

It is essential to compare the above galactic tau neutrino flux with the flux of atmospheric tau neutrinos. The intrinsic atmospheric tau neutrino flux has been calculated for $E \leq 10^6$ GeV [7]. In this work, we extend the calculation up to $E \leq 10^{11}$ GeV. Such an extension requires the input of cosmic-ray flux spectrum for an energy range beyond that considered in Ref. [7]. Furthermore, for a greater neutrino energy, the solutions of cascade equations relevant to the neutrino production behave differently. For the oscillated ν_τ flux, it is interesting to note that the oscillation length for $\nu_\mu \rightarrow \nu_\tau$ for the energy range $10^3 \leq E/\text{GeV} \leq 10^{11}$ is much greater than the thickness of the

* E-mail: athar@phys.cts.nthu.edu.tw

† E-mail: cheung@phys.cts.nthu.edu.tw

‡ E-mail: glin@cc.nctu.edu.tw

§ E-mail: geny.py86g@nctu.edu.tw

earth atmosphere. Hence the oscillated atmospheric ν_τ flux in this case is highly suppressed.

One may argue that the interaction of the high-energy cosmic-rays with the ubiquitous cosmic microwave background (CMB) photons present in cosmos ($p\gamma$ rather than pp interactions) could also be an important source for high-energy astrophysical tau neutrinos. The center-of-mass energy (\sqrt{s}) needed to produce a τ lepton and a ν_τ is at least ~ 1.8 GeV. In a collision between a proton with an energy E_p and a CMB photon with an energy $E_{\gamma_{\text{CMB}}}$, the center-of-mass energy squared of the system satisfies $m_p^2 < s < 4E_p E_{\gamma_{\text{CMB}}} + m_p^2$. Since the peak of the CMB photon flux spectrum with a temperature ~ 2.7 K is at about $2.3 \cdot 10^{-4}$ eV, it requires a very energetic proton with $E_p \gtrsim 2.5 \cdot 10^{12}$ GeV in order to produce a $\tau\nu_\tau$ pair. Thus, the contribution of the intrinsic tau neutrino flux from the interaction between the cosmic proton and the CMB photon is negligible, unless we are considering extremely high-energy protons, beyond the presently observed highest energy cosmic-rays [8]. To compute the oscillated ν_τ flux in this case, we consider the non-tau neutrino flux generated by the $p\gamma$ interaction via the Δ resonance, commonly referred to as the Greisen-Zatsepin-Kuzmin (GZK) cutoff interaction, which assumes that the proton travels a cosmological distance [9]. A recent calculation of the intrinsic non-tau GZK neutrino flux indicates that this flux peaks typically at $E \sim 10^9$ GeV [10], beyond the reach of presently operating high-energy neutrino telescopes such as AMANDA and Baikal experiments [1]. This flux decreases for $E < 10^9$ GeV. In fact, it falls below the intrinsic non-tau galactic-plane neutrino flux for $E \leq 5 \cdot 10^7$ GeV. The neutrino flavor oscillations of the intrinsic non-tau GZK neutrinos into tau neutrinos result in a ν_τ flux comparable to the original non-tau neutrino flux [11]. Therefore, in the absence (or smallness) of tau neutrino flux from other possible extra-galactic astrophysical sites, the only source of high-energy tau neutrinos besides the atmospheric background is from our (plane of) galaxy, typically for $10^3 \leq E/\text{GeV} \leq 5 \cdot 10^7$. This is an energy range to be explored by the above high-energy neutrino telescopes in the near future.

The organization of the paper is as follows. In Section II, we discuss the calculation of intrinsic high-energy tau neutrino flux from our galaxy, including the description of the flux formula, the galaxy model, and the various tau neutrino production channels taken into account in the calculation. Although this flux will be shown small, we shall go through some details of the calculation since they are also useful for the calculation in the next section. In Section III, we present our result on the intrinsic atmospheric ν_τ flux and compare it with the galactic one. In Section IV, we discuss the effects of neutrino flavor mixing, which are used to construct the oscillated ν_τ fluxes from the galaxy and the earth atmosphere respectively. The total galactic ν_τ flux (the sum of intrinsic and oscillated fluxes) is compared to its atmospheric counterpart, and the dominant energy range for the former flux is identified. We also mention the currently envisaged prospects for identifying the high-energy tau neutrinos. We summarize in Section V.

II. THE INTRINSIC GALACTIC TAU NEUTRINO FLUX

A. The tau-neutrino flux formula and the galaxy model

We use the following formula for computing the ν_τ flux:

$$\frac{dN_{\nu_\tau}}{dE} = \int_E^\infty dE_p \phi_p(E_p) f(E_p) \frac{dn_{pp \rightarrow \nu_\tau + Y}}{dE}. \quad (1)$$

In the above equation, E is the tau neutrino energy and the cosmic-ray flux spectrum, $\phi_p(E_p)$, is given by [12]

$$\phi_p(E_p) = \begin{cases} 1.7 (E_p/\text{GeV})^{-2.7} & \text{for } E_p < E_0, \\ 174 (E_p/\text{GeV})^{-3} & \text{for } E_p \geq E_0, \end{cases} \quad (2)$$

where $E_0 = 5 \cdot 10^6$ GeV and $\phi_p(E_p)$ is in units of $\text{cm}^{-2} \text{s}^{-1} \text{sr}^{-1} \text{GeV}^{-1}$. We assume directional isotropy in $\phi_p(E_p)$ for the above energy range. The function $f(E_p)$ is equal to $R/\lambda_{pp}(E_p)$, where $\lambda_{pp}(E_p) = (\sigma_{pp}^{\text{incl}} n_p)^{-1}$ is the pp interaction length and R is a representative distance in the galaxy along the galactic plane. The target particles are taken to be protons with a constant number density of 1 cm^{-3} and R is taken to be ~ 10 kpc, where $1 \text{ pc} \simeq 3 \cdot 10^{18} \text{ cm}$. The $\sigma_{pp}^{\text{incl}}$ is the total inelastic pp cross section. Since the high-energy protons traverse a distance R much shorter than the proton interaction length, the proton flux spectrum $\phi_p(E_p)$ is assumed to be constant over the distance R . Furthermore, we calculate the intrinsic tau neutrino flux along the galactic plane only to obtain the maximal expected tau neutrino flux. The matter density decreases exponentially in the direction orthogonal to the galactic plane, therefore the amount of intrinsic tau neutrino flux decreases by approximately two orders of magnitude for the energy range of our interest. For further details, see Ingelman and Thunman in Ref. [5]. The function $f(E_p)$ in Eq. (1) basically gives the number of inelastic pp collisions in the distance R , while the distribution dn/dE is the differential cross section normalized by $\sigma_{pp}^{\text{incl}}$, i.e.,

$$\frac{dn_{pp \rightarrow \nu_\tau + Y}}{dE} = \frac{1}{\sigma_{pp}^{\text{incl}}} \frac{d\sigma_{pp \rightarrow \nu_\tau + Y}}{dE}. \quad (3)$$

The above distribution gives the fraction of inelastic pp interactions that goes into ν_τ 's. We can now simplify Eq. (1) into

$$\frac{dN_{\nu_\tau}}{dE} = Rn_p \int_E^\infty dE_p \phi_p(E_p) \frac{d\sigma_{pp \rightarrow \nu_\tau + Y}}{dE}. \quad (4)$$

It is clear that the task of computing dN_{ν_τ}/dE relies on the evaluation of the differential cross section $d\sigma/dE$ in pp interactions. In this work, we include all major production channels of tau neutrinos, namely, via the D_s meson, b -hadron, $t\bar{t}$, W^* , and Z^* . In general, the symbol ν_τ shall be used to account for the contribution of ν_τ and $\bar{\nu}_\tau$ unless otherwise mentioned. We note that the heavy intermediate states, such as the D_s meson, b -hadrons and other heavier states, decay (into ν_τ) before they interact with other particles in the galactic plane. This is due to the rather small matter density of the medium and the large distance between the proton source and the earth. Before we proceed, let us remark that the intrinsic tau neutrino production by the galactic $p\gamma$ interactions is suppressed relative to that in the galactic pp interaction, because $n_\gamma \ll n_p$ for the energy range of interest to us [13].

B. Tau neutrino production

1. Via D_s mesons

The lightest meson that can decay into a $\tau\nu_\tau$ pair is the D_s meson. It was pointed out that the production and the decay of D_s meson is the major production channel for tau neutrinos in the AGN [14]. We expect the same will be true for galactic tau neutrinos. The D_s meson decays into a charged τ lepton and a ν_τ . The charged τ lepton subsequently decays into the second ν_τ plus other particles, which can be one prong or three prong. The kinematics of the τ lepton decay is treated by the Monte Carlo technique. For simplicity, we assume that the τ lepton decays into a ν_τ and a particle Y with the mass m_Y satisfying $0.1 \text{ GeV} < m_Y < m_\tau - 0.1 \text{ GeV}$. Consequently, the second ν_τ is much more *energetic* than the first one because the D_s mass is only slightly larger than m_τ . We take the branching ratio $B(D_s \rightarrow \tau^+\nu_\tau)$ as $\simeq 0.074$ [15].

We now turn to the production of D_s mesons. Here, we employ two approaches to calculate the production of D_s mesons: (i) the perturbative QCD (PQCD) and (ii) the quark-gluon string model (QGSM). In the PQCD approach, we use the leading-order result for $pp \rightarrow c\bar{c}$:

$$\sigma(pp \rightarrow c\bar{c}) = \sum_{ij} \int \int dx_1 dx_2 f_{i/p}(x_1) f_{j/p}(x_2) \hat{\sigma}(ij \rightarrow c\bar{c}), \quad (5)$$

where $f_{i/p}(x)$ are the parton distribution functions (we use the CTEQv5 [16]), while the parton subprocesses are $q\bar{q}, gg \rightarrow c\bar{c}$. We use a K factor, $K = 2$, to account for the NLO corrections [17]. The matrix elements for these subprocesses can be found in Appendix A. The c or \bar{c} then undergoes fragmentation into the D_s meson, which we model by the Peterson fragmentation function [18] with $\epsilon \simeq 0.029$ [19] (see Appendix A). The probability $f_{c \rightarrow D_s}$ of a *charm* quark fragmenting into a D_s is 0.19 [19] (we have added the $f_{c \rightarrow D_s}$ and $f_{\bar{c} \rightarrow D_s}$). Typically, a fraction z ($z < 1$) of the charm-quark energy is transferred to the D_s meson so that the energy spectrum of D_s is softer than that of the charm quark.

The QGSM approach is nonperturbative and is based on the string fragmentation. It contains a number of parameters determined by experiments [20]. The production cross section of the D_s meson is given by the sum of n -pomeron terms

$$\frac{d\sigma^{D_s}(s, x)}{dx} \approx \frac{1}{x^2 + x_\perp^2} \sum_{n=1}^{\infty} \sigma_n^{pp}(s) \phi_n^{D_s}(s, x), \quad (6)$$

where $x = 2p_{\parallel}/\sqrt{s}$ and $x_\perp = 2\sqrt{(m_{D_s}^2 + p_\perp^2)}/s$. The functions $\sigma_n^{pp}(s)$ and $\phi_n^{D_s}(s, x)$ are given in Appendix B.

A comparison of these two approaches for D_s meson is shown in Fig. 1. The dashed line in the figure is the spectrum of the injected proton flux given by Eq. (2). The ν_τ spectra calculated by these two approaches agree well with each other for $E \leq 10^6$ GeV. Beyond this energy, the QGSM approach gives a relatively harder spectrum. In fact, this behavior was already seen in the $d\sigma/dx$ distribution. Nevertheless, in the region where the two approaches differ, the tau neutrino flux is already small. To our knowledge, the heaviest meson production that the QGSM has been applied to is the D_s meson production. The current highest energy collider experiment for D_s meson production is at the FERMILAB TEVATRON with $\sqrt{s} = 1.8 \cdot 10^3$ GeV, which corresponds to an $E_p \sim 1.7 \cdot 10^6$ GeV, as $s \sim 2m_p E_p$ in our setting. Note that up to this \sqrt{s} , the agreement between the two approaches is quite good, according to Fig.

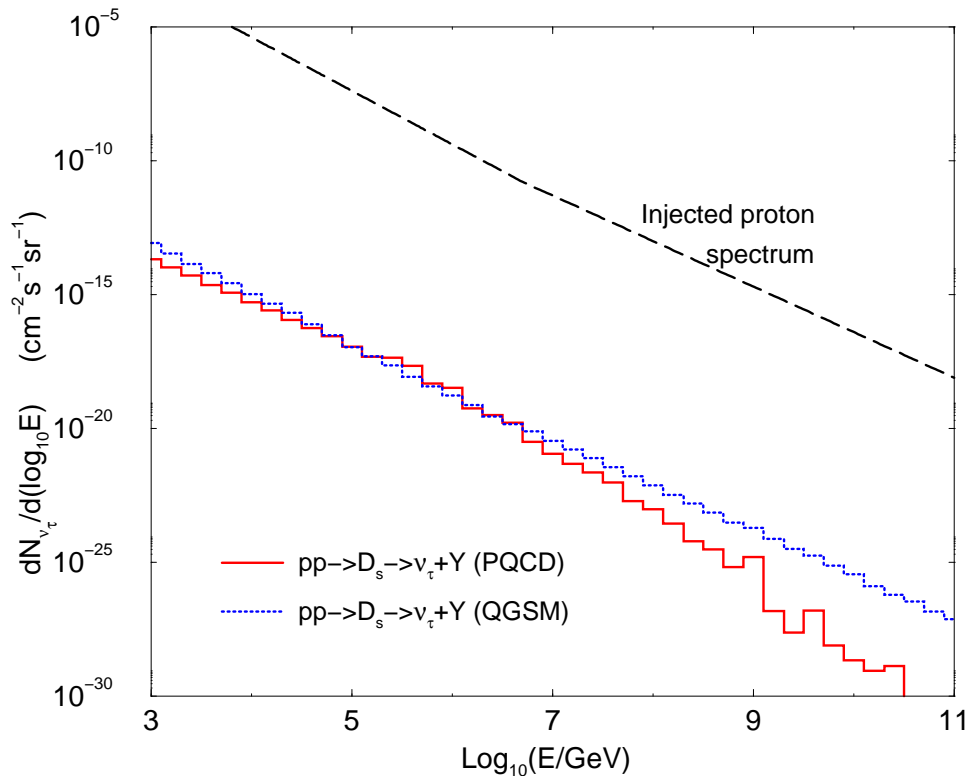


FIG. 1: A comparison between the PQCD and QGSM approach to the energy spectrum of the intrinsic galactic ν_τ flux coming from the D_s meson. The thick dashed curve is the injected proton flux spectrum given by Eq. (2).

1. We have used a factorization scale $Q^2 = \hat{s}/4$ and the one-loop running strong coupling constant α_s with the value $\alpha_s(Q^2 = M_Z^2) = 0.118$, and the $m_c = 1.35$ GeV.

An important quantity in the neutrino flux calculation is the average fraction of the injected proton energy being transferred to the tau neutrino, i.e., the ratio $r \equiv E/E_p$. The average value of r is given either by the mean

$$\langle r \rangle = \frac{\int r \left(\frac{d\sigma}{dE} \right) dr}{\int \left(\frac{d\sigma}{dE} \right) dr}, \quad (7)$$

or by the value of r at which the distribution $d\sigma/dE$ attains the peak. We have found that both averages of r are very close to each other. The $\langle r \rangle$ ranges from $5 \cdot 10^{-3}$ to $5 \cdot 10^{-7}$ for E_p from 10^3 to 10^{11} GeV for the production channel $pp \rightarrow c\bar{c} \rightarrow D_s + Y \rightarrow \nu_\tau + Y$, using the PQCD approach. The higher the injected proton energy, the smaller is the fraction of the incident E_p that goes into hadrons.

2. Via $b\bar{b}$, $t\bar{t}$, W^* and Z^*

The production of $b\bar{b}$ and $t\bar{t}$ in pp interactions can be calculated quite reliably by the PQCD approach, similar to the calculation of $c\bar{c}$. The relevant matrix elements, including the ones for W^* and Z^* , are listed in Appendix A. The results¹ are shown in Fig. 2. A few observations can be drawn from the figure [21]. (i) The production via D_s mesons dominates for $E \leq 10^9$ GeV, followed by b -hadrons, W^* , Z^* , and $t\bar{t}$ respectively. (ii) For $E \geq 10^9$ GeV all these

¹ After taking into account the sources of uncertainties such as values of m_c , m_b , m_t , R , n_p , etc., we estimate that our calculation of the intrinsic galactic ν_τ flux is reliable within an order of magnitude.

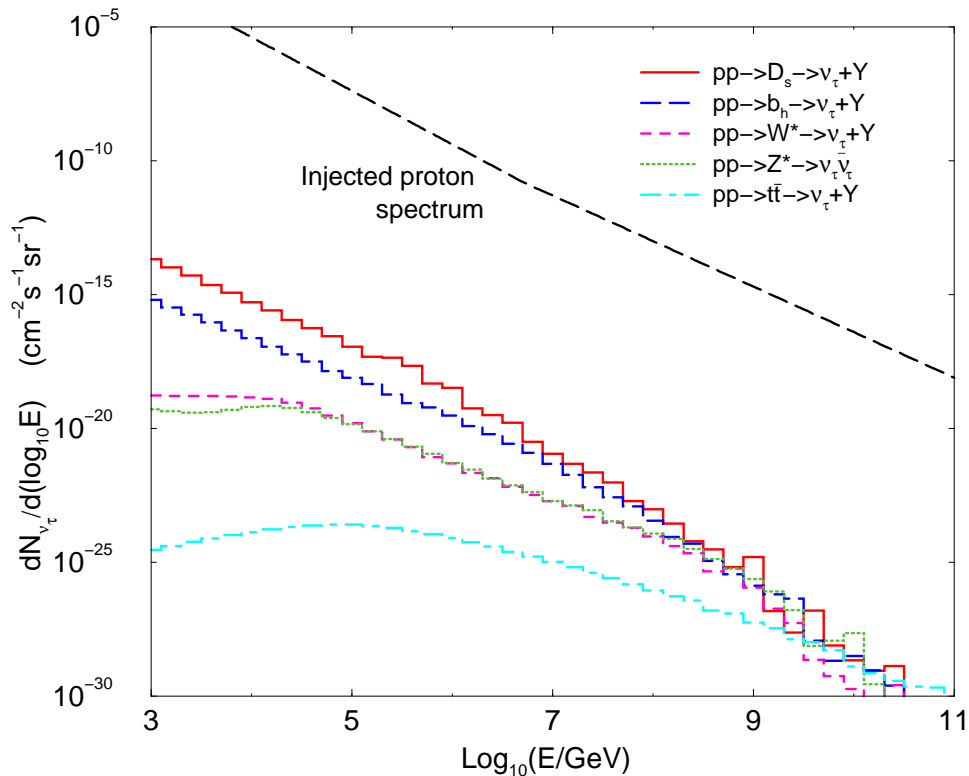


FIG. 2: Intrinsic galactic tau neutrino flux calculated via various intermediate states and channels: D_s , b -hadron, W^* , Z^* , and $t\bar{t}$. The injected proton flux spectrum is also shown.

production channels become *comparable*. (iii) The intrinsic tau neutrino flux is about 10 – 12 orders of magnitude smaller than the injected proton flux.

III. THE INTRINSIC ATMOSPHERIC TAU NEUTRINO FLUX

The earth atmosphere is an interesting extra-terrestrial site where the basic pp interaction occurs in the form of a pA collision with A the nuclei present in the earth atmosphere. Incidentally, it is the only known nearby extra-terrestrial site from where the intrinsic neutrinos are observed as a result of high-energy cosmic-ray interactions.

We have calculated the downward and horizontal intrinsic atmospheric ν_{τ} flux for the energy range $10^3 \leq E/\text{GeV} \leq 10^{11}$. We used the nonperturbative QCD approach mentioned in the last section to model the production of D_s mesons in pA interactions. We have used the $\phi_p(E_p)$ given by Eq. (2) and the Z -moment description for the calculation of intrinsic tau neutrino flux, which is appropriate for a varying target density medium [22]. Since the tau neutrino flux is determined by the flux of D_s meson, we briefly discuss the cascade equation for the D_s flux. In general, we have [22]

$$\frac{d\phi_{D_s}}{dX} = -\frac{\phi_{D_s}}{\lambda_{D_s}} - \frac{\phi_{D_s}}{\rho d_{D_s}} + Z_{D_s D_s} \frac{\phi_{D_s}}{\lambda_{D_s}} + Z_{p D_s} \frac{\phi_p}{\lambda_p}, \quad (8)$$

where X is the slant depth, i.e., the amount of atmosphere (in g/cm^2) traversed by the D_s meson ($X = 0$ at the top of the atmosphere), $\phi_p(E, X)$ and $\phi_{D_s}(E, X)$ are the fluxes of protons and D_s mesons respectively. The λ_{D_s} and d_{D_s} are the interaction thickness (in g/cm^2) and the decay length of the D_s meson respectively. Finally, the Z -moments $Z_{p D_s}$ and $Z_{D_s D_s}$ describe the effectiveness of generating D_s meson from the higher-energy protons and D_s mesons respectively. We have

$$\begin{aligned} Z_{p D_s}(E) &= \int_E^\infty dE' \frac{\phi_p(E', 0)}{\phi_p(E, 0)} \frac{\lambda_p(E)}{\lambda_p(E')} \frac{dn_{pA \rightarrow D_s + Y}(E, E')}{dE}, \\ Z_{D_s D_s}(E) &= \int_E^\infty dE' \frac{\phi_{D_s}(E', 0)}{\phi_{D_s}(E, 0)} \frac{\lambda_{D_s}(E)}{\lambda_{D_s}(E')} \frac{dn_{D_s A \rightarrow D_s + Y}(E, E')}{dE}, \end{aligned} \quad (9)$$

where $dn_{pA \rightarrow D_s + Y}/dE$ and $dn_{D_s A \rightarrow D_s + Y}/dE$ are defined according to Eq. (3). We note that Eq. (8) should be solved together with the cascade equation governing the propagation of high-energy cosmic-ray protons. In fact, the proton flux equation can be easily solved such that

$$\phi_p(E, X) \approx \exp\left(-\frac{X}{\Lambda_p}\right) \phi_p(E, 0), \quad (10)$$

where $\Lambda_p \equiv \lambda_p/(1 - Z_{pp})$ is the proton attenuation length with λ_p the proton interaction thickness (in g/cm²) and the Z_{pp} given by

$$Z_{pp}(E) = \int_E^\infty dE' \frac{\phi_p(E', 0)}{\phi_p(E, 0)} \frac{\lambda_p(E)}{\lambda_p(E')} \frac{dn_{pA \rightarrow p+Y}(E, E')}{dE}. \quad (11)$$

An analytic solution of Eq. (8) can be obtained for either the low or the high energy limit. Such limits are characterized by whether the D_s decays before it interacts with the medium or vice versa. The critical energy separating the two limits is approximately $\sim 8.5 \cdot 10^7$ GeV. In the low energy limit, we disregard the first and third terms in the R.H.S. of Eq. (8). On the other hand, one can drop the second term in the high energy limit. With ϕ_{D_s} determined, the ν_τ flux can be calculated by considering the decay $D_s \rightarrow \nu_\tau \tau$ and the subsequent decay $\tau \rightarrow \nu_\tau + Y$ as treated in Section II. We first obtain two ν_τ fluxes, valid for low and high energy limits respectively, in terms of Z -moments and then interpolate the two fluxes. A complete numerical solution without the interpolation is given in a separate work [23].

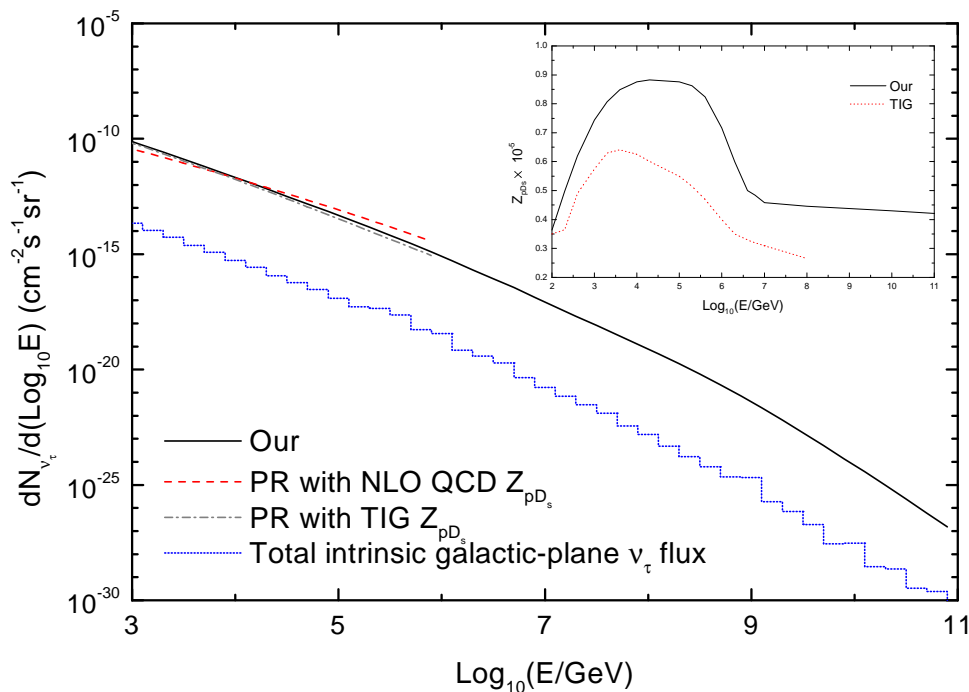


FIG. 3: Intrinsic horizontal ν_τ flux via production and decay of the D_s meson in the earth atmosphere. For $10^3 \leq E/\text{GeV} \leq 10^6$, the results by PR are also shown. In the inset, we compare our calculated Z_{pD_s} with the one given by rescaling TIG's Z_{pD^0} . The total intrinsic galactic-plane tau neutrino flux is also shown.

In Fig. 3, we show our result for the intrinsic atmospheric ν_τ flux along the horizontal direction. For comparison, the results by Pasquali and Reno (PR) [7], valid for $10^3 \leq E/\text{GeV} \leq 10^6$, are also shown. The ν_τ flux along all the other direction is small. For example², the downward ν_τ flux is about 8 times smaller than the horizontal one

² The upward going high-energy ν_τ with a energy $E \geq 10^4$ GeV is degraded in energy to about $E \leq 10^3$ GeV after crossing the earth.

for $E \geq 10^8$ GeV. We remark that the major uncertainty for determining the above ν_τ flux is the Z -moment Z_{pD_s} . In Ref. [7], the authors calculate Z_{pD_s} using two different approaches, which then give rise to different results for the ν_τ flux. The first approach is based upon next-to-leading order (NLO) perturbative QCD [24], while the second approach rescales the Z_{pD^0} given by the PYTHIA [25] calculation of Thunman, Ingelman, and Gondolo (TIG) [26]. In the inset of Fig. 3, we also show our calculated Z_{pD_s} in comparison with the one given by rescaling TIG's result for Z_{pD^0} . We do not show the Z_{pD_s} obtained by NLO perturbative QCD since it is not explicitly given in Ref. [7].

IV. EFFECTS OF OSCILLATIONS AND PROSPECTS FOR OBSERVATIONS

In the context of two neutrino flavors, ν_μ and ν_τ , the total ν_τ flux, $dN_{\nu_\tau}^{\text{tot}}/d(\log_{10} E)$, is given by [27]

$$dN_{\nu_\tau}^{\text{tot}}/d(\log_{10} E) = P \cdot dN_{\nu_\mu}/d(\log_{10} E) + (1 - P) \cdot dN_{\nu_\tau}/d(\log_{10} E). \quad (12)$$

Here $P \equiv P(\nu_\mu \rightarrow \nu_\tau) = \sin^2 2\theta \cdot \sin^2(l/l_{\text{osc}})$. The neutrino flavor oscillation length for $\nu_\mu \rightarrow \nu_\tau$ is $l_{\text{osc}} \sim (E/\delta m^2)$. For $10^3 \leq E/\text{GeV} \leq 10^{11}$ and with $\delta m^2 \sim 10^{-3} \text{ eV}^2$, we obtain $10^{-8} \leq l_{\text{osc}}/\text{pc} \leq 1$. We assume maximal flavor mixing between ν_μ and ν_τ .

For intrinsic neutrinos produced along the galactic plane, we take $dN_{\nu_\mu}/d(\log_{10} E)$ given by Ingelman and Thunman in Ref. [5] by extrapolating it up to $E \leq 10^{11}$ GeV, whereas for $dN_{\nu_\tau}/d(\log_{10} E)$, we use our results obtained in Section II. For galactic-plane neutrinos, we note that $l_{\text{osc}} \ll l$, where $l \sim 5$ kpc is the typical average distance the intrinsic high-energy muon neutrinos traverse after being produced in our galaxy. Eq. (12) then implies that, on the average, half of the muon neutrino flux will be oscillated into tau neutrino flux, reducing its intrinsic level to one half.

For downward going neutrinos produced in the earth atmosphere, we take $l \simeq 20$ km as an example. We use the (prompt) $dN_{\nu_\mu}/d(\log_{10} E)$ given in [28], whereas for $dN_{\nu_\tau}/d(\log_{10} E)$, we use our results obtained in Section III. For horizontal and upward going atmospheric neutrinos, $l \sim 10^3 - 10^4$ km. Here, $l_{\text{osc}} \gg l$, and so the intrinsic atmospheric tau neutrino flux dominates over the oscillated one for $E \geq 10^3$ GeV, essentially irrespective of the incident direction. We present these results in Fig. 4, along with the GZK oscillated tau neutrino flux briefly mentioned in Section I. For the GZK neutrinos, $l \geq \text{Mpc}$ and $dN_{\nu_\mu}/d(\log_{10} E)$ is taken from Ref. [10]. From the figure, we note that the galactic-plane oscillated ν_τ flux *dominates* over the intrinsic atmospheric ν_τ flux for $E \leq 5 \cdot 10^7$ GeV, whereas the GZK oscillated tau neutrino flux dominates for $E \geq 5 \cdot 10^7$ GeV.

A prospective search for high-energy tau neutrinos can be done by appropriately utilizing the characteristic τ lepton range in deep inelastic (charged current) tau-neutrino-nucleon interactions, in addition to the attempt of observing the associated showers. For E close to $6 \cdot 10^6$ GeV, the (anti electron) neutrino-electron resonant scattering is also available to the search for (secondary) high-energy tau neutrinos [29]. The main advantages of using the latter channel are that the neutrino flavor in the initial state is least affected by neutrino flavor oscillations and that this cross section is free from theoretical uncertainties [30]. The appropriate utilization of the characteristic τ lepton range in both interaction channels not only helps to identify the incident neutrino flavor but also helps to bracket the incident neutrino energy as well, at least in principle.

For downward going or near horizontal high-energy tau neutrinos, the deep inelastic neutrino-nucleon scattering, occurring near or inside the detector, produces two (hadronic) showers [31]. The first shower is due to a charged-current neutrino-nucleon deep inelastic scattering, whereas the second shower is due to the (hadronic) decay of the associated τ lepton produced in the first shower. It might be possible for the proposed large neutrino telescopes such as IceCube to constrain the two showers simultaneously for $10^6 \leq E/\text{GeV} \leq 10^7$, depending on the achievable shower separation capabilities [32] (see, also, [1]). Here, the two showers develop mainly in ice. Using the same shower separation criteria as given in [32], we note that the $\sim (100 \text{ m})^3$ proposed neutrino detector, commonly called the megaton detector [33], may constrain the two showers separated by ≥ 10 m, typically for $5 \cdot 10^5 \leq E/\text{GeV} \leq 10^6$. The two nearly horizontal showers may also possibly be contained in a large surface area detector array such as Pierre Auger, typically for $5 \cdot 10^8 \leq E/\text{GeV} \leq 10^9$ [34]. In contrast to previous situations, here the two showers develop mainly in air. Several different suggestions have recently been made to measure only one shower, which is due to the τ lepton decay, typically for $10^8 < E/\text{GeV} < 10^{10}$, while the first shower is considered to be mainly absorbed in the earth [35]. The upward going high-energy tau neutrinos with $E \geq 10^4$ GeV, on the other hand, may avoid earth shadowing to a certain extent because of the characteristic τ lepton range, unlike the upward going electron and muon neutrinos, and may appear as a rather small pile up of ν_l ($l = e, \mu, \text{ and } \tau$) with $E \sim 10^3$ GeV [36, 37]. However, the empirical determination of incident tau neutrino energy seems rather challenging here.

The above studies indicate that for a rather large range of tau neutrino energy, a prospective search may be carried out. The event rate in each experimental configuration is directly proportional to the incident ν_τ flux and the effective area of the detector concerned. Presently, no direct empirical upper bounds (or observations) for high-energy tau neutrinos exist.

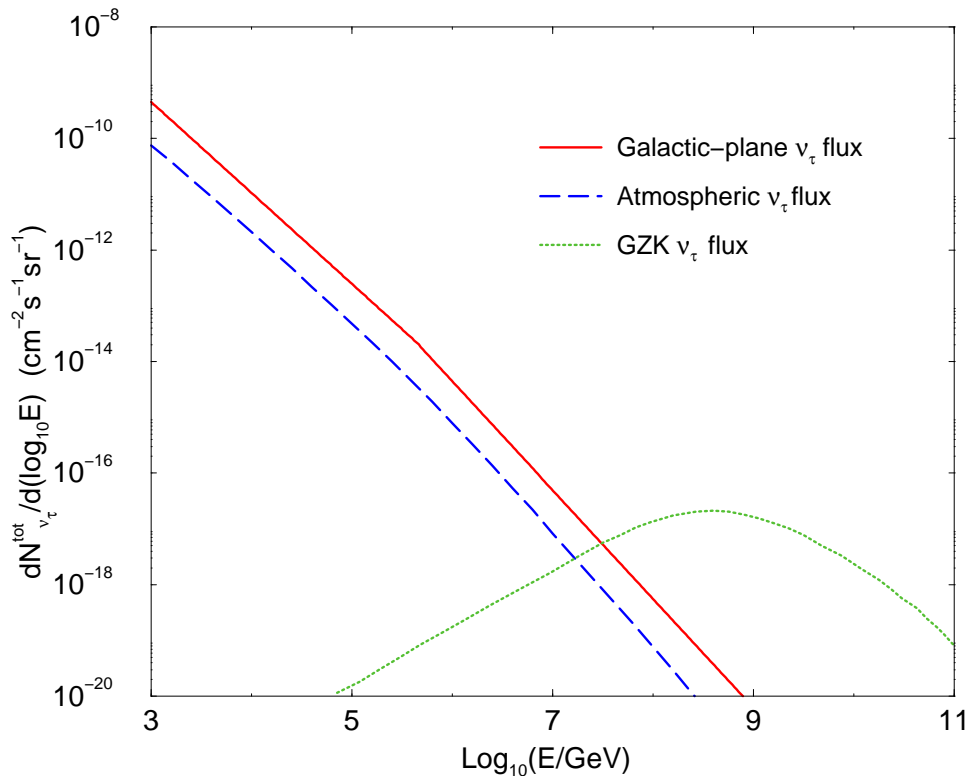


FIG. 4: Galactic-plane, horizontal atmospheric and GZK tau neutrino fluxes under the assumption of neutrino flavor oscillations.

To have an idea of the event rate, let us consider the downward going high-energy tau neutrinos originating from the galactic-plane due to neutrino flavor oscillations. The flux of such neutrinos has been given in Fig. 4. Following Ref. [32], we note that these galactic tau neutrinos give a representative event rate of ≤ 1 per year per steradian for two separable and contained showers with $E \sim 10^6$ GeV in a km^3 volume neutrino telescope such as the proposed IceCube.

V. DISCUSSION AND CONCLUSIONS

We have calculated the ν_{τ} flux due to pp interactions in our galaxy. This flux consists of intrinsic tau neutrino flux and that arising from the oscillations of muon neutrinos. We note that the latter flux is dominant over the former by four to five orders of magnitude for the considered neutrino energy range. From Fig. 4, one can see that the main background for the search of high-energy extra-galactic tau neutrino is due to the muon neutrinos produced in the galactic-plane, which then oscillate into tau neutrinos. Such a flux dominates for $10^3 \leq E/\text{GeV} \leq 5 \cdot 10^7$. Therefore it is clear that searching for extra-galactic tau neutrinos orthogonal to the galactic-plane is more prospective.

In the calculation of galactic tau neutrino flux, we have used a simplified model of matter distribution along our galactic plane to obtain the maximal intrinsic tau neutrino flux. We have explicitly calculated the contribution of heavier states such as $b\bar{b}$, $t\bar{t}$ as well as W^* and Z^* in addition to the more conventional D_s channel to the intrinsic tau neutrino flux. We have estimated the average fraction of the incident cosmic-ray energy that goes into tau neutrinos and found it to be less than 1%. The contributions from $b\bar{b}$, $t\bar{t}$, W^* and Z^* channels are comparable to D_s for $E \geq 10^9$ GeV. For D_s channel, we have used both perturbative and nonperturbative QCD approaches.

We have extended a previous calculation of intrinsic atmospheric ν_{τ} flux from $E \leq 10^6$ GeV up to $E \leq 10^{11}$ GeV. Here, we used the nonperturbative QCD approach to calculate the production of D_s mesons in pA interactions. In comparison with the intrinsic galactic-plane ν_{τ} flux, it is large. However, since the distance between the detector and the neutrino source in the galactic plane is sufficiently large, the neutrino flavor oscillations of non-tau neutrinos into tau neutrinos makes the eventual tau neutrino flux along the galactic plane greater than the atmospheric tau neutrino flux for $10^3 \leq E/\text{GeV} \leq 5 \cdot 10^7$. However, the intrinsic atmospheric ν_{τ} flux dominates over the oscillated galactic ν_{τ} flux in the direction orthogonal to the galactic plane. We have also briefly mentioned the presently envisaged

prospects for observations. In summary, we have completed the compilation of all definite sources of tau neutrino flux, i.e., those from our galaxy and from the earth atmosphere. Such a compilation is needed before one conducts the search for tau neutrinos from extra-galactic sources.

Acknowledgments

H.A. and K.C. are supported in part by the Physics Division of National Center for Theoretical Sciences under a grant from the National Science Council of Taiwan. G.L.L. and J.J.T. are supported by the National Science Council of R.O.C. under the grant number NSC90-2112-M009-023.

-
- [1] For a recent review article, see, for instance, F. Halzen, arXiv:astro-ph/0111059 and references therein.
- [2] Y. Fukuda *et al.* [Super-Kamiokande Collaboration], Phys. Rev. Lett. 81 (1998) 1562.
- [3] S. Fukuda *et al.* [Super-Kamiokande Collaboration], Phys. Rev. Lett. 85 (2000) 3999.
- [4] K. Kodama *et al.* [DONUT Collaboration], Phys. Lett. B 504 (2001) 218; J. Sielaff [DONUT Collaboration], arXiv:hep-ex/0105042.
- [5] F. W. Stecker, Astrophys. J. 228 (1979) 919; G. Domokos, B. Elliott and S. Kovesi-Domokos, J. Phys. G 19 (1993) 899; V. S. Berezhinsky, T. K. Gaisser, F. Halzen and T. Stanev, Astropart. Phys. 1 (1993) 281; G. Ingelman and M. Thunman, arXiv:hep-ph/9604286.
- [6] A. De Rujula, E. Fernandez and J. J. Gomez-Cadenas, Nucl. Phys. B 405 (1993) 80; M. C. Gonzalez-Garcia and J. J. Gomez-Cadenas, Phys. Rev. D 55 (1997) 1297.
- [7] L. Pasquali and M. H. Reno, Phys. Rev. D 59 (1999) 093003.
- [8] M. Nagano and A. A. Watson, Rev. Mod. Phys. 72 (2000) 689.
- [9] K. Greisen, Phys. Rev. Lett. 16 (1966) 748; G. T. Zatsepin and V. A. Kuzmin, JETP Lett. 4 (1966) 78 [Pisma Zh. Eksp. Teor. Fiz. 4 (1966) 114].
- [10] R. Engel, D. Seckel and T. Stanev, Phys. Rev. D 64 (2001) 093010.
- [11] H. Athar, arXiv:hep-ph/0008121.
- [12] T. H. Burnett *et al.* [JACEE Collaboration], Astrophys. J. Lett. 349 (1990) L25.
- [13] For an estimate of galactic n_γ , see, Berezhinsky *et al.*, in Ref. [5].
- [14] H. Athar, Nucl. Phys. Proc. Suppl. 76 (1999) 419.
- [15] D. E. Groom *et al.* [Particle Data Group Collaboration], Eur. Phys. J. C 15 (2000) 1.
- [16] H. L. Lai *et al.* [CTEQ Collaboration], Eur. Phys. J. C 12 (2000) 375.
- [17] See, for instance, P. Nason, S. Dawson and R. K. Ellis, Nucl. Phys. B 327 (1989) 49 [Erratum-ibid. B 335 (1989) 260].
- [18] C. Peterson, D. Schlatter, I. Schmitt and P. M. Zerwas, Phys. Rev. D 27 (1983) 105.
- [19] R. Barate *et al.* [ALEPH Collaboration], Eur. Phys. J. C 16 (2000) 597.
- [20] A. B. Kaidalov, Phys. Lett. B 116 (1982) 459; A. B. Kaidalov and O. I. Piskunova, Sov. J. Nucl. Phys. 43 (1986) 994 [Yad. Fiz. 43 (1986) 1545]; G. G. Arakelian and P. E. Volkovitsky, Z. Phys. A 353 (1995) 87; G. H. Arakelian, Phys. Atom. Nucl. 61 (1998) 1570 [Yad. Fiz. 61 (1998) 1682]; G. H. Arakelian and S. S. Eremian, Phys. Atom. Nucl. 62 (199) 1724 [Yad. Fiz. 62 (1999) 1851]. See, also, M. C. Gonzalez-Garcia and J. J. Gomez-Cadenas, in Ref. [6].
- [21] For a more detailed discussion, see K. Cheung, in: H. Athar, G.-L. Lin and K.-W. Ng (Eds.), Proceedings of the First NCTS Workshop on Astroparticle Physics, 2001, Kenting (Taiwan) [to be published].
- [22] T. K. Gaisser, Cosmic Rays And Particle Physics, Cambridge University Press, NewYork, 1990.
- [23] J.-J. Tseng, Ph.D. Thesis, NCTU, 2002 (in preparation).
- [24] S. Frixione, M. L. Mangano, P. Nason, and G. Ridolfi, Nucl. Phys. B 431 (1994) 453.
- [25] T. Sjostrand, Comput. Phys. Commun. 82 (1994) 74.
- [26] M. Thunman, G. Ingelman and P. Gondolo, Astropart. Phys. 5 (1996) 309.
- [27] See, for instance, H. Athar, M. Jezabek and O. Yasuda, Phys. Rev. D 62 (2000) 103007 and references therein.
- [28] L. V. Volkova and G. T. Zatsepin, Phys. Atom. Nucl. 64 (2001) 266 [Yad. Fiz. 64 (2001) 313].
- [29] D. Fargion, arXiv:astro-ph/9704205.
- [30] H. Athar and G.-L. Lin, arXiv:hep-ph/0108204; *ibid.*, arXiv:hep-ph/0201026.
- [31] J. G. Learned and S. Pakvasa, Astropart. Phys. 3 (1995) 267.
- [32] H. Athar, Astropart. Phys. 14 (2000) 217; H. Athar, G. Parente and E. Zas, Phys. Rev. D 62 (2000) 093010.
- [33] See, for instance, H. Chen *et al.* [VLBL Study Group H2B-1 Collaboration], arXiv:hep-ph/0104266.
- [34] H. Athar, arXiv:hep-ph/0004083.
- [35] D. Fargion, arXiv:astro-ph/0002453; X. Bertou, P. Billoir, O. Deligny, C. Lachaud and A. Letessier-Selvon, arXiv:astro-ph/0104452; J. L. Feng, P. Fisher, F. Wilczek and T. M. Yu, arXiv:hep-ph/0105067; A. Kusenko and T. Weiler, arXiv:hep-ph/0106071.
- [36] F. Halzen and D. Saltzberg, Phys. Rev. Lett. 81 (1998) 4305.

[37] F. Becattini and S. Bottai, *Astropart. Phys.* 15 (2001) 323; S. Iyer Dutta, M. H. Reno and I. Sarcevic, arXiv:hep-ph/0110245 and references therein; J. F. Beacom, P. Crotty and E. W. Kolb, arXiv:astro-ph/0111482.

APPENDIX A: FORMULAS FOR PQCD

In this appendix, we list the matrix element squared for the subprocesses of $pp \rightarrow Q\bar{Q}$, where $Q = c, b, t$, used in the PQCD calculation.

$$\begin{aligned}
\frac{d\hat{\sigma}}{d\cos\theta^*}(q\bar{q} \rightarrow Q\bar{Q}) &= \frac{g_s^4\beta}{72\pi\hat{s}^3} \left[(m_Q^2 - \hat{t})^2 + (m_Q^2 - \hat{u})^2 + 2\hat{s}m_Q^2 \right], \\
\frac{d\hat{\sigma}}{d\cos\theta^*}(gg \rightarrow Q\bar{Q}) &= \frac{g_s^4\beta}{768\pi\hat{s}} \left\{ \frac{4}{(\hat{t} - m_Q^2)^2} (-m_Q^4 - 3m_Q^2\hat{t} - m_Q^2\hat{u} + \hat{u}\hat{t}) \right. \\
&\quad + \frac{4}{(\hat{u} - m_Q^2)^2} (-m_Q^4 - 3m_Q^2\hat{u} - m_Q^2\hat{t} + \hat{u}\hat{t}) \\
&\quad + \frac{m_Q^2}{(\hat{u} - m_Q^2)(\hat{t} - m_Q^2)} (2m_Q^2 + \hat{t} + \hat{u}) + 18\frac{1}{\hat{s}^2} (m_Q^4 - m_Q^2(\hat{t} + \hat{u}) + \hat{t}\hat{u}) \\
&\quad \left. + \frac{9}{\hat{t} - m_Q^2} \frac{1}{\hat{s}} (m_Q^4 - 2m_Q^2\hat{t} + \hat{u}\hat{t}) + \frac{9}{\hat{u} - m_Q^2} \frac{1}{\hat{s}} (m_Q^4 - 2m_Q^2\hat{u} + \hat{u}\hat{t}) \right\}, \tag{A1}
\end{aligned}$$

where $g_s^2 = 4\pi\alpha_s$, $\beta = \sqrt{1 - (4m_Q^2/\hat{s})}$ and $\hat{s}, \hat{t}, \hat{u}$ are the usual Mandelstem variables with $\hat{t} - m_Q^2 = -(\hat{s}/2)(1 - \beta \cos\theta^*)$.

The subprocesses for high-energy tau neutrino production via W^* and Z^* are $q\bar{q}' \rightarrow W^* \rightarrow \tau^\pm \nu_\tau$ and $q\bar{q} \rightarrow Z^* \rightarrow \nu_\tau \bar{\nu}_\tau$. The spin- and color-averaged amplitude squared for these subprocesses are given by

$$\begin{aligned}
\overline{|\mathcal{M}(u\bar{d} \rightarrow W^* \rightarrow \tau^+ \nu_\tau)|} &= \frac{g^4}{12} \frac{1}{(\hat{s} - m_W^2)^2 + \Gamma_W^2 m_W^2} \hat{t}(\hat{t} - m_\tau^2), \\
\overline{|\mathcal{M}(d\bar{u} \rightarrow W^* \rightarrow \tau^- \bar{\nu}_\tau)|} &= \frac{g^4}{12} \frac{1}{(\hat{s} - m_W^2)^2 + \Gamma_W^2 m_W^2} \hat{u}(\hat{u} - m_\tau^2), \\
\overline{|\mathcal{M}(q\bar{q} \rightarrow Z^* \rightarrow \nu_\tau \bar{\nu}_\tau)|} &= \frac{g^4}{3\cos^4\theta_w} \frac{1}{(\hat{s} - m_Z^2)^2 + \Gamma_Z^2 m_Z^2} \left[(g_L^\nu g_L^q)^2 \hat{u}^2 + (g_L^\nu g_R^q)^2 \hat{t}^2 \right], \tag{A2}
\end{aligned}$$

where $g_L^f = T_{3f} - Q_f \sin^2\theta_w$ and θ_w is the weak mixing angle, T_{3f} is the third component of the weak isospin and Q_f is the electric charge in units of proton charge of the fermion f .

The Peterson fragmentation function is given by

$$D_{Q \rightarrow h_Q}(z) = N \frac{z(1-z)^2}{[(1-z)^2 + \epsilon z]^2}, \tag{A3}$$

where N is the normalization constant and ϵ is given in the text.

APPENDIX B: FORMULAS FOR QGSM

In Eq. (6), the functions $\sigma_n^{pp}(s)$ and $\phi_n^{D_s}(s, x)$ are given as follows:

$$\phi_n^{D_s}(s, x) = a_0^{D_s} \left[F_{qq}^{D_s}(x_+, n) F_q^{D_s}(x_-, n) + F_q^{D_s}(x_+, n) F_{qq}^{D_s}(x_-, n) + 2(n-1) F_{sea}^{D_s}(x_+, n) F_{sea}^{D_s}(x_-, n) \right], \tag{B1}$$

where

$$F_q^{D_s}(x, n) = \frac{2}{3} \int_x^1 dx_1 f_p^u(x_1, n) G_u^{D_s} \left(\frac{x}{x_1} \right) + \frac{1}{3} \int_x^1 dx_1 f_p^d(x_1, n) G_d^{D_s} \left(\frac{x}{x_1} \right), \tag{B2}$$

$$F_{qq}^{D_s}(x, n) = \frac{2}{3} \int_x^1 dx_1 f_p^{ud}(x_1, n) G_{ud}^{D_s} \left(\frac{x}{x_1} \right) + \frac{1}{3} \int_x^1 dx_1 f_p^{uu}(x_1, n) G_{uu}^{D_s} \left(\frac{x}{x_1} \right), \tag{B3}$$

$$\begin{aligned}
F_{sea}^{D_s}(x, n) = & \frac{1}{4 + 2\delta_s + 2\delta_c} \left\{ \int_x^1 dx_1 f_p^{u_{sea}}(x_1, n) \left[G_u^{D_s} \left(\frac{x}{x_1} \right) + G_{\bar{u}}^{D_s} \left(\frac{x}{x_1} \right) \right] \right. \\
& + \int_x^1 dx_1 f_p^{d_{sea}}(x_1, n) \left[G_d^{D_s} \left(\frac{x}{x_1} \right) + G_{\bar{d}}^{D_s} \left(\frac{x}{x_1} \right) \right] \\
& + \delta_s \int_x^1 dx_1 f_p^{s_{sea}}(x_1, n) \left[G_s^{D_s} \left(\frac{x}{x_1} \right) + G_{\bar{s}}^{D_s} \left(\frac{x}{x_1} \right) \right] \\
& \left. + \delta_c \int_x^1 dx_1 f_p^{c_{sea}}(x_1, n) \left[G_c^{D_s} \left(\frac{x}{x_1} \right) + G_{\bar{c}}^{D_s} \left(\frac{x}{x_1} \right) \right] \right\}. \tag{B4}
\end{aligned}$$

In the above, $f_p^i(x, n)$'s are the distribution functions describing the n -Pomeron distribution functions of quarks or diquarks ($i = u, d, uu\dots$) with a fraction of energy x from the proton, and $G_i^h(z)$'s are the fragmentation functions of the quark or diquark chain into a hadron h which carries a fraction z of its energy.

The list of the $f_p^i(x, n)$ are given by

$$\begin{aligned}
f_p^u(x, n) &= \frac{\Gamma(1 + n - 2\alpha_N)}{\Gamma(1 - \alpha_R) \Gamma(\alpha_R - 2\alpha_N + n)} \times x^{-\alpha_R} (1 - x)^{\alpha_R - 2\alpha_N + (n-1)}, \\
&= f_p^{u_{sea}}, \\
f_p^d(x, n) &= \frac{\Gamma(2 + n - 2\alpha_N)}{\Gamma(1 - \alpha_R) \Gamma(\alpha_R - 2\alpha_N + n + 1)} \times x^{-\alpha_R} (1 - x)^{\alpha_R - 2\alpha_N + n}, \\
&= f_p^{d_{sea}}, \\
f_p^{uu}(x, n) &= \frac{\Gamma(2 + n - 2\alpha_N)}{\Gamma(-\alpha_R + n) \Gamma(\alpha_R - 2\alpha_N + 1)} \times x^{\alpha_R - 2\alpha_N + 1} (1 - x)^{-\alpha_R + (n-1)}, \\
f_p^{ud}(x, n) &= \frac{\Gamma(1 + n - 2\alpha_N)}{\Gamma(-\alpha_R + n) \Gamma(\alpha_R - 2\alpha_N + 2)} \times x^{\alpha_R - 2\alpha_N} (1 - x)^{-\alpha_R + (n-1)}, \\
f_p^{s_{sea}}(x, n) &= \frac{\Gamma(1 + n + 2\alpha_R - 2\alpha_N - 2\alpha_\phi)}{\Gamma(1 - \alpha_\phi) \Gamma(2\alpha_R - 2\alpha_N + n - \alpha_\phi)} \times x^{-\alpha_\phi} (1 - x)^{2\alpha_R - 2\alpha_N + (n-1) - \alpha_\phi}, \\
f_p^{c_{sea}}(x, n) &= \frac{\Gamma(1 + n + 2\alpha_R - 2\alpha_N - 2\alpha_\psi)}{\Gamma(1 - \alpha_\psi) \Gamma(2\alpha_R - 2\alpha_N + n - \alpha_\psi)} \times x^{-\alpha_\psi} (1 - x)^{2\alpha_R - 2\alpha_N + (n-1) - \alpha_\psi},
\end{aligned}$$

where Γ is the usual Gamma function.

The list of the $G_i^{D_s^\pm}(z)$ are given by

$$\begin{aligned}
G_{u, \bar{u}, d, \bar{d}}^{D_s^\pm}(z) &= (1 - z)^{\lambda - \alpha_\psi + 2 - \alpha_R - \alpha_\phi}, \\
G_{uu, ud}^{D_s^\pm}(z) &= (1 - z)^{\lambda - \alpha_\psi + \alpha_R - 2\alpha_N - \alpha_\phi + 2}, \\
G_s^{D_s^+}(z) &= (1 - z)^{\lambda - \alpha_\psi + 2(1 - \alpha_\phi)}, \\
&= G_{\bar{s}}^{D_s^-}(z), \\
G_s^{D_s^-}(z) &= (1 - z)^{\lambda - \alpha_\psi} \times (1 + a_1 z^2), \\
&= G_{\bar{s}}^{D_s^+}(z), \\
G_{c, \bar{c}}^{D_s^\pm}(z) &= z^{1 - \alpha_\psi} (1 - z)^{\lambda - \alpha_\phi}.
\end{aligned}$$

In the above, the input parameters are as follows:

$$\begin{aligned}
\alpha_R &= 0.5, \\
\alpha_N &= -0.5, \\
\alpha_\phi &= 0, \\
\alpha_\psi &= -2.18, \\
\lambda &= 0.5, \\
\delta_s &= 0.25,
\end{aligned}$$

$$\begin{aligned}
a_0^{D_s} &= 0.0007, \\
a_1 &= 5, \\
\delta_c &= 0 \text{ (0.01), if charm sea contribution is turned off (on).}
\end{aligned}$$

The function $\sigma_n^{pp}(s)$ is given by the following formulas:

$$\sigma_n^{pp}(\xi) = \frac{\sigma_p}{n z} \left(1 - \exp(-z) \sum_{k=0}^{n-1} \frac{z^k}{k!} \right), \quad (\text{B5})$$

where

$$\begin{aligned}
\xi &= \ln \left(\frac{s}{1 \text{ (GeV)}^2} \right), \\
z &= \frac{2C \gamma_p}{R^2 + \alpha_p' \xi} \exp(\xi \Delta), \\
\sigma_p &= 8\pi \gamma_p \exp(\xi \Delta).
\end{aligned}$$

The best fit parameters are as follows :

(i) for $\sqrt{s} \leq 10^3 \text{ GeV}$

$$\begin{aligned}
\gamma_p &= 3.64 \text{ (GeV)}^{-2}, \\
R^2 &= 3.56 \text{ (GeV)}^{-2}, \\
\alpha_p' &= 0.25 \text{ (GeV)}^{-2}, \\
C &= 1.5, \\
\Delta &= 0.07.
\end{aligned}$$

(ii) for $\sqrt{s} \geq 10^3 \text{ GeV}$

$$\begin{aligned}
\gamma_p &= 1.77 \text{ (GeV)}^{-2}, \\
R^2 &= 3.18 \text{ (GeV)}^{-2}, \\
\alpha_p' &= 0.25 \text{ (GeV)}^{-2}, \\
C &= 1.5, \\
\Delta &= 0.139.
\end{aligned}$$